Constraining the effect of image resolution in digital rock physics without segmentation

Eric J. Goldfarb, Ken Ikeda, and Nicola Tisato, The University of Texas at Austin, Jackson School of Geosciences*

Summary

Digital rock physics (DRP) is used to estimate physical properties of rocks by means of digital models. Conventional digital rock physics requires very high resolution images, as grains and pores need to be well resolved in order to assign each voxel the properties of an endmember. Using the targeted method, which does not require segmentation, voxels that capture a mixture of pore and grain are assigned the properties of the mixture by means of an effective medium theory. The targeted method, therefore, does not require resolving individual grain boundaries, and lower resolution scanning is possible. Here we show the results of segmentation-less DRP where four Berea sandstone samples were scanned with a resolution at 40 microns per voxel, and two of the samples were also scanned at 60 and 80 microns per voxel. Density, porosity and elastic properties were estimated for each scan, then compared to laboratory measurements. At a first order, the rocks scanned at multiple resolutions show no obvious effect on property estimation compared to laboratory measurements. The low resolution scans were computationally efficient, and accuracy was not compromised. This abstract provides further validation of the targeted DRP methodology.

Introduction

When creating large subsurface models, geoscientists typically use non-invasive geophysical techniques that sacrifice a degree of accuracy in exchange for cost. Digging and drilling is more accurate, but very expensive. Common methods include gravity, seismic, or electromagnetic surveying. Interpretation typically involves inverse models, which have a measurable degree of uncertainty. Physical samples such as those collected from nearby outcrops, core or even drill cuttings are invaluable to calibrate models. Rock type, porosity, density, and seismic velocity are properties of interest for resource or civil engineers. Ground truth, or results from rocks can de-risk a model, as the ability to physically measure properties lessens the "guess work" from non-unique inverse models.

Characterizing these properties is part of the discipline of rock physics. Using numerical simulation to estimate these properties is called digital rock physics (DRP). Numerical estimation of physical properties is desirable for several reasons. Laboratory measurements of velocity, elastic properties, or microscopy involves cutting samples into a specific shape. This is irreversible, and often not ideal for rare samples like drilling cores. It can also be difficult to measure multiple properties on the identical section of rock; for example, we cannot measure porosity accurately from a thin section that we use for petrography. If a digital model exists, it can be numerically cropped without physically harming the sample. Because digital tests are non-damaging, multiple tests can be conducted on the same region of the sample. In addition, physical laboratory work is expensive and time consuming. The methodology behind DRP will likely never fully replace the laboratory. However, it is possible that in the future, rather than just processing a few samples in the laboratory, it may be preferable to process a mixture that involves less laboratory samples and many DRP samples. This would likely be associated to a decrease in costs.

Typically, DRP has a workflow that requires assuming or capturing the structure of a sample in order to create a digital model. For example, the structural makeup for a sedimentary arenite could be simplified in a model to be spherically packed grains surrounded by air (e.g. Kehhm et al., 2001). To create a more accurate model, real information can be captured in two dimensions using microscopy; increasingly, three dimensional models have been captured using Computed Tomography (CT) scanning (Espinoza et al., 2016). This abstract will focus on this last type of technique.

Computed Tomography records the attenuation of X-rays passing through a sample. A three-dimensional model can be created where each resolvable cubic sub domain is a three-dimensional pixel, or voxel. Each voxel is defined by a value, known as CT number, that represents the amount of relative attenuation at that location. As a first order approximation, dense regions attenuate X-rays more than less dense regions. Dense regions therefore yield higher CT number (Landis and Keane, 2010). Relationships between CT attenuation, density, porosity, and stiffness have been proposed (e.g. Taud et al., 2004; Tanaka et al., 2011; Verga et al., 2014; Li et al., 2015).

Conventional DRP assigns each voxel to a mineral phase or pore space based off its CT number. Dense voxels will be assigned as grains, and light voxels as air. Using quartz arenite as an example, voxels will be assigned identities of quartz or air, and given physical properties to represent these regions. If resolution is not high enough to resolve small features such as grain contacts, information from pore and grain are "blended" as a single value and the partial volume effect occurs (Ketcham and Carlson, 2001). In order to segment the dataset, the value will be rounded to

10.1190/segam2018-2997871.1

an endmember - even though it is not. In addition, segmentation is uncertain due to its arbitrary nature (Andrä et al., 2013). Different people may treat voxels with the partial volume effect as different endmembers. The process also assumes all grains are pristine mineral phases, when they are probably not. Calling minerals pristine obliterates the information from microfractures and impurities, which are often sub micrometric in size. This causes physical properties to be over predicted (Madonna et al., 2012). In order to limit this problem, extremely high dataset resolution is needed. This creates a problem, as a sugar-cube sized sample translates into a model of terabytes in size; this becomes impractical to process.

The representative elementary volume (REV) is defined as the smallest required sample size that can accurately represent the sample lithology. Given the high resolution and dataset size requirements of segmentation, it might prove computationally difficult to model a sample that is large enough to be an REV (Kelly et al., 2016). The basis of this abstract uses an alternative to segmented DRP, known as the “targeted” or “segmentation-less” method (Tisato and Spikes, 2016; Goldfarb et. al 2017; Ikeda et. al 2017). Here we show that by means of targeted DRP it is possible to capture models at lower resolutions without compromising the quality of physical property estimation. Using targeted DRP, physically larger samples could be processed at lower resolutions. This allows the scanning of more representative samples without a corresponding increase in the size of the dataset.

Theory

Madonna et al (2012) used DRP on a segmented model at very high resolution (~3 microns per voxel) and overestimated elastic properties. However, by manually lowering the values near grain boundaries from "pristine" mineral properties, they were able to simulate realistic values for their DRP model. They concluded that grain contacts, impurities and microfractures are critical, as rocks are more than a compilation of pristine minerals. In other words, even at very high resolutions, the segmentation process is too binary for real world conditions.

This observation helps explain the targeted method, which also lowers elastic properties from pristine minerals. The method does so in a less arbitrary manner. Targeted DRP workflow (Figure 1) begins with the creation of a three-dimensional model of a rock, captured by a CT scanner. The model consists of voxels, where each voxel has a value representing X-rays attenuation at that location. Physical objects of known density, or targets, are also scanned alongside the rock. Measuring the CT number in a target region, and pairing it with its known density, provides values that can be used to make a calibration curve unique to the scan. Using this curve, each voxel’s value (CT number) in the imagery dataset can be converted to density (Mull,1984).

In rocks where grains are a consistent material with a known density, a porosity model can be inferred from the density model. A linearly inverse relationship is defined between porosity and density, where voxels with a density equal or greater to that of the frame (e.g. for the case of a clean sandstone, use quartz) have a porosity of 0%. Voxels with a density of air are assigned 100% porosity. A linear function is then used to define voxels with densities between the value of the frame and the value of air.

Given a known rock frame type, effective medium theory is used to estimate elastic properties of individual voxels. Voxels containing partial volumes (i.e. porosity between 1% and 99%) are recognized as a mixture of grain and pore. Using effective medium theory, they are assigned the respective elastic properties of a mixture. Goldfarb et al. (2017) empirically compared several effective medium theories, each which outputs a slightly different model of bulk and shear modulus. The authors made recommendations for targeted DRP which are incorporated in the Method section of this abstract.

The targeted method is preferential to segmentation at low resolutions. Targeted CT accounts for impurities and partial volumes, as it does not round voxels to be endmembers. While decreasing resolution will increase the number of partial volume captured in voxels, this is not an issue if effective medium theory is used to describe mixtures, and not segmenting to an endmember.

The standard elastic velocity equations require inputs of density, bulk modulus and shear modulus (Mavko et al., 2009). As these are now available in the DRP workflow, velocity models for P and S waves can be created. Next, numerical simulations of ultrasonic wave propagation can be performed by means of the finite difference method (Bohlen, 2002). After simulating the propagation of waves through a numerical velocity model, a seismogram can be created. Wave speeds are estimated by dividing the “length” of the digital sample model by the picked first arrival from the simulated seismogram.

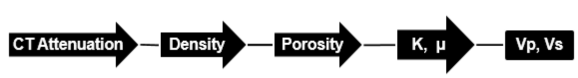

Figure 1: Workflow for estimation of rock and mineral properties. CT attenuation is recorded. Attenuation values can be converted to density with a density/attenuation conversion curve from scanned targets. Porosity can be estimated from the inverse relationship to density. Elastic moduli are calculated according to an effective medium

theory. Velocity estimations are obtained from finite difference wave propagation simulations.

Goldfarb et al., (2017) tested several approaches when using effective medium theory. They had an arenite sample with endmembers of quartz and air, and a known porosity and density. First, they calculated elastic properties of the entire sample by means of effective medium theories and found that this largely over-predicted the rock properties. This is comparable to acquiring a scan of the sample at extremely low resolution, such that the entire rock can be considered a single voxel. Then, they used targeted DRP and applied the same effective medium theories to individual voxels (resolution of 40 microns per voxel). This approach was more accurate than the previous method, but their work still lacked a systematic study on the effect of CT resolution on the final result.

Resolution can be seen as a balance between quality of information and ease of data processing. For quick processing, resolution should be as low as possible. However, when it comes to estimating rock properties, conventional segmentation needs resolution to be as high as possible in order to minimize voxels with partial volumes. In segmented DRP, this is because small fractures and partial volumes will be rounded to endmembers. However, with targeted CT scanning, the partial volume effect is no longer detrimental. With this method, voxels can represent mixtures of grains and pores, and therefore, the negative effect from rounding a large voxel to an endmember can be mitigated.

There is not a common resolution value that will work for each rock type; rather, there might be a relationship between the number of voxels that capture individual grains and accuracy of the segmentation-less method. The ideal resolution will likely be similar for alike lithologies and available technology. A scan at one resolution may be suitable to describe grain to grain contacts in a coarse sandstone, but it will not be enough to resolve mineral contacts in a siltstone or shale.

Method

We cut four Berea sandstone plugs, grinded the end faces, and dried the samples in an oven. The plugs were 2.5 cm in diameter, images can be found in Figure 2, and physical properties in Table 1. Densities were calculated with a scale and a caliper with precisions of 0.001g and 0.01 mm, respectively. Sample porosities were measured by means of a helium pycnometer (AccuPyc II 1340 V2.01). We used the pulse receiver method with ultrasonic piezoelectric transducers (Olympus Videoscan) with a 1 MHz frequency to propagate waves through the samples (Birch, 1961). Wavelets for P and S waves were recorded by means of a digital oscilloscope (Rigol DS1104) and we manually picked first arrival times.

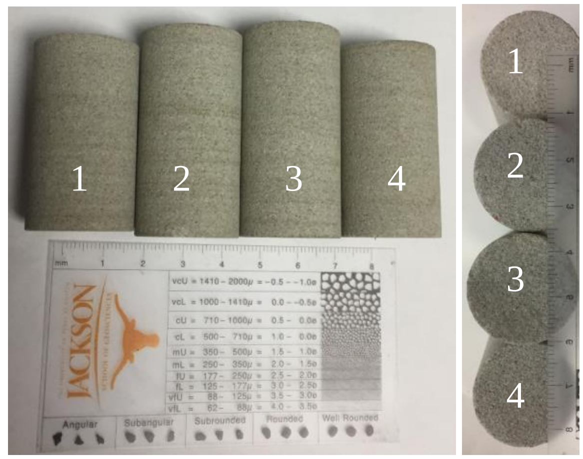

Figure 2: Images of the length and width of the Berea sandstone samples.

All samples were scanned with a micro computed tomography scanner (Nikon XT H 225) at a resolution of 40 microns per voxel, so that rock and elastic properties could be estimated with DRP. In addition, samples 1 and 2 were also scanned at 60 and 80 microns per voxel, in order to assess the effects of resolution on physical property estimation. Samples were rotated 1440 increments to reach a full rotation, with a projection taken at each increment. Beam energy was ~125 kV, and energy was ~138 μA. Minor beam hardening corrections were applied. After reconstruction, two dimensional slices of 16 bit voxels were created and saved as TIFF images. Figure 3 is an example of a TIFF image at several resolutions.

The rock was scanned using three targets: air, polycarbonate, and the rock itself (densities of 1.225, 1246, and 2120 kg/m^3 respectively).

We estimated the rock elastic properties and density of the samples (see Theory, and Goldfarb et al., 2017). For an effective medium theory, we used a modified Voigt-Reuss-Hill average with a critical porosity of 0.35. According to the model, when porosity is very low, elastic properties are simplified to be near half of that of a pure mineral. This is ideal for three reasons:

- It is unlikely that any grain in the mineral is pristine. Considering the erosion, transport, burial, lithification, and exposure processes, grains are typically damaged. This method lowers properties to represent such damage.
- This model was used in Goldfarb et al., 2017. We have not changed it, in order to use predictive DRP, and not simply fit a model to each unique rock;

- The modelled results continue to fit well empirically.

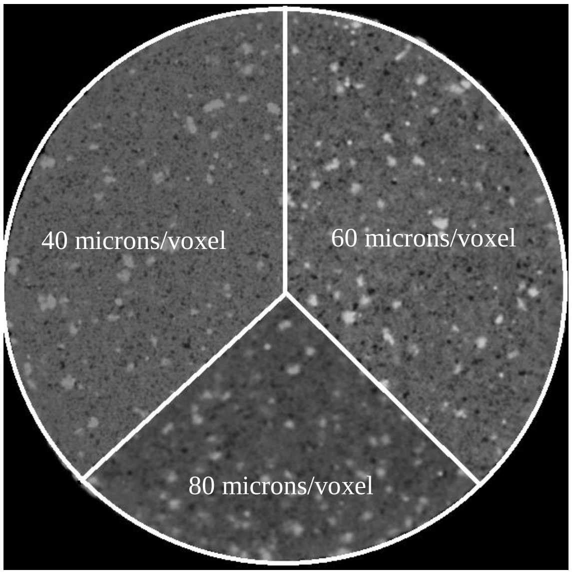

Figure 3: CT greyscale images at three resolutions. Diameter is 2.5 cm. Darker colour represents less attenuation.

Results

Laboratory results, and measured physical properties are summarized in Table 1. Figures 4 and 5 summarize estimation of properties form targeted DRP with comparison to laboratory values. At first approximation, results from targeted DRP estimation are close to laboratory measurements, irrespective of CT resolution.

Table 1: Properties measured in the laboratory for all samples.

Property	Error	Units	Sample Number			
			1	2	3	4
Length	±0.07	mm	45.00	50.11	51.98	47.98
Density	±20	kg/m^3	2120	2120	2130	2120
Porosity	±1.1	%	20.9	20.4	20.2	21.3
P wave velocity	±100	m/s	3040	3093	3113	2908
S wave velocity	±175	m/s	2000	1920	1920	1999
P to S wave ratio	±0.08	none	1.52	1.61	1.62	1.45

Estimation of properties for sample 1 appear to become more accurate at lower resolutions, while accuracy for sample 2 does not improve at lower resolutions; this leaves the effect on precision as inconclusive. Density results for all resolutions come close to laboratory measurements (within 2%). Porosity estimates are generally accurate (within 5% of laboratory value).

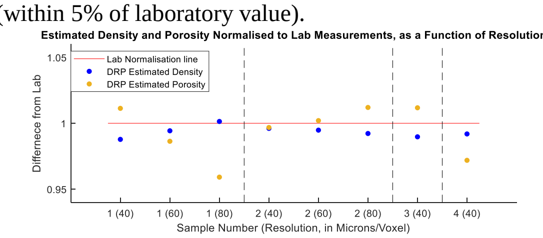

Figure 1: A comparison between estimation of density and porosity from DRP to laboratory measurements.

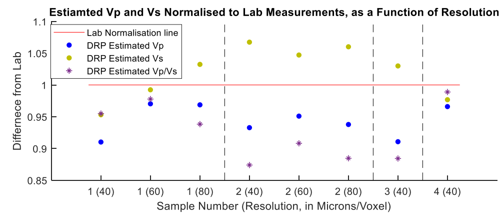

Figure 2: A comparison between seismic velocities estimated with DRP and laboratory measurements.

Estimates of V_p and V_s have mismatch from the laboratory measurements of less than 9% and change little with resolution. V_s values tend to over predict the laboratory results, and show less difference to the laboratory value. V_p tends to under predict laboratory values. V_p/V_s ratio for DRP estimation yields values between 1.43 and 1.49 for all samples. Castagna et al., (1985) suggests that for dry Berea sandstone, a value of 1.5 is typical.

Conclusion

We have performed further validation of targeted CT scanning for multiple Berea sandstone samples. We have found that density, porosity, and velocity estimation is similar to laboratory measurements.

There does not appear to be a strong trend with any rock or elastic property that would indicate deteriorating with the lowering of scan resolution scan. This is largely related to the use of effective medium theory, where voxels with partial volumes of grain and pore can be represented as such. This is promising, as it would suggest that larger samples can be scanned, with the intent of scanning more representative volumes allowing also easier data processing. Work is continuing with this methodology on more complex lithologies and additional conditions.

Acknowledgment
Thanks to Mathew Ramos, Colin Shroeder, Brandon Minton, Nicolas Espinoza, Rich Ketcham, Maša Prodanović, Daniella Rempe, Kyle Spikes, and Jessie Maisano for help with various stages of the project.

10.1190/segam2018-2997871.1

REFERENCES

Andrä, H., N. Combaret, J. Dvorkin, E. Glatt, J. Han, M. Kabel, Y. Keehm, F. Krzikalla, M. Lee, and C. Madonna, 2013, Digital rock physics benchmarks—Part I: Imaging and segmentation: Computers & Geosciences, **50**, 25–32, https://doi.org/10.1016/j.cageo.2012.09.005.

Birch, F., 1961, The velocity of compressional waves in rocks to 10 kilobars: 2: Journal of Geophysical Research, **66**, 2199–2224, https://doi.org/10.1029/JZ066i007p02199.

Bohlen, T., 2002, Parallel 3-D viscoelastic finite difference seismic modeling: Computers & Geosciences, **28**, 887–899, https://doi.org/10.1016/S0098-3004(02)00006-7.

Castagna, J. P., M. L. Batzle, and R. L. Eastwood, 1985, Relationships between compressional-wave and shear-wave velocities in clastic silicate rocks: Geophysics, **50**, 571–581, https://doi.org/10.1190/1.1441933.

Espinoza, D. N., I. Shovkun, O. Makni, and N. Lenoir, 2016, Natural and induced fractures in coal cores imaged through X-ray computed microtomography—Impact on desorption time: International Journal of Coal Geology, **154**, 165–175, https://doi.org/10.1016/j.coal.2015.12.012.

Goldfarb, E., K. Ikeda, and N. Tisato, 2017, Segmentationless digital rock physics using different effective medium theories: 87th Annual International Meeting, SEG, Expanded Abstracts, 3908–3913, https://doi.org/10.1190/segam2017-17792957.1.

Ikeda, K., E. Goldfarb, and N. Tisato, 2017, Static elastic properties of Berea sandstone by means of segmentation-less digital rock physics: 87th Annual International Meeting, SEG, Expanded Abstracts, 3914–3919, https://doi.org/10.1190/segam2017-17789805.1.

Keehm, Y., T. Mukerji, and A. Nur, 2001, Computational rock physics at the pore scale: Transport properties and diagenesis in realistic pore geometries: The Leading Edge, **20**, 180–183, https://doi.org/10.1190/1.1438904.

Kelly, S., H. El-Sobky, C. Torres-Verdín, and M. T. Balhoff, 2016, Assessing the utility of FIB-SEM images for shale digital rock physics: Advances in Water Resources, **95**, 302–316, https://doi.org/10.1016/j.advwatres.2015.06.010.

Ketcham, R. A., and W. D. Carlson, 2001, Acquisition, optimization and interpretation of X-ray computed tomographic imagery: Applications to the geosciences. Computers & Geosciences, **27**, 381–400, https://doi.org/10.1016/S0098-3004(00)00116-3.

Landis, E. N., and D. T. Keane, 2010, X-ray microtomography: Materials Characterization, **61**, 1305–1316, https://doi.org/10.1016/j.matchar.2010.09.012.

Li, L., I. Larsen, and R. M. Holt, 2015, Laboratory observation and micromechanics-based modelling of sandstone on different scales: Rock Mechanics and Rock Engineering, **48**, 1407–1422, https://doi.org/10.1007/s00603-014-0642-5.

Madonna, C., B. S. Almqvist, and E. H. Saenger, 2012, Digital rock physics: Numerical prediction of pressure-dependent ultrasonic velocities using micro-CT imaging: Geophysical Journal International, **189**, 1475–1482, https://doi.org/10.1111/j.1365-246X.2012.05437.x.

Mavko, G., T. Mukerji, and J. Dvorkin, 2009, The rock physics handbook: Tools for seismic analysis of porous media: Cambridge University Press.

Mull, R. T., 1984, Mass estimates by computed tomography: physical density from CT numbers: American Journal of Roentgenology, **143**, 1101–1104, https://doi.org/10.2214/ajr.143.5.1101.

Tanaka, A., T. Nakano, and K. Ikehara, 2011, X-ray computerized tomography analysis and density estimation using a sediment core from the Challenger Mound area in the Porcupine Seabight, off Western Ireland: Earth, Planets and Space, **63**, 103–110, https://doi.org/10.5047/eps.2010.12.006.

Taud, H., R. Martinez-Angeles, J. Parrot, and L. Hernandez-Escobedo, 2005, Porosity estimation method by X-ray computed tomography: Journal of Petroleum Science and Engineering, **47**, 209–217, https://doi.org/10.1016/j.petrol.2005.03.009.

Tisato, N., and K. Spikes, 2016, Computation of effective elastic properties from digital images without segmentation: 86th Annual International Meeting, SEG, Expanded Abstracts, 3256–3260, https://doi.org/10.1190/segam2016-13947820.1.

Vega, B., A. Dutta, and A. R. Kovscek, 2014, CT imaging of low-permeability, dual-porosity systems using high X-ray contrast gas: Transport in Porous Media, **101**, 81–97, https://doi.org/10.1007/s11242-013-0232-0.

10.1190/segam2018-2997871.1